Parametric decay of oblique whistler waves in the Earth's magnetosphere: 2-D PIC simulations

Yangguang Ke, Xinliang Gao, Quanming Lu, Yufei Hao, and Shui Wang

Parametric decay of oblique whistler waves in the Earth's magnetosphere: 2-D PIC simulations

Yangguang Ke,[1,2] Xinliang Gao,[1,2,a)] Quanming Lu,[1,2] Yufei Hao,[1,2] and Shui Wang[1,2]
[1]*CAS Key Laboratory of Geospace Environment, Department of Geophysics and Planetary Science, University of Science and Technology of China, Hefei 230026, China*
[2]*Collaborative Innovation Center of Astronautical Science and Technology, Harbin 150001, China*

Whistler mode waves in the Earth's magnetosphere have already been widely investigated in the linear or quasi-linear regime, but there is still lack of research on nonlinear physical processes. In this paper, with a 2-D PIC simulation model, we have studied the parametric decay of oblique whistler waves for the first time. The parametric decay of an oblique whistler wave first occurs along its propagating direction, which involves a backward daughter whistler wave and a forward ion acoustic mode. This is quite similar to the parametric decay of parallel whistler waves in 1-D simulations. Interestingly, the parametric decay will then take place along the perpendicular direction, which can generate a family of daughter whistler waves along the perpendicular direction with the nearly same parallel wave number. Meanwhile, the highly oblique whistler waves will also be excited during this perpendicular decay, whose wave normal angle can even reach up to the resonant cone angle. Moreover, the parametric decay tends to be stronger for the pump whistler wave with a larger frequency or larger amplitude. But the growth rate of the parametric decay has little change when the wave normal angle of the pump whistler wave varies within a limited range. Interestingly, parallel whistler waves can also experience the similar decay process, which may suggest that the parametric decay of whistler waves should be a multi-dimensional process in nature. During the decay process, the generated ion acoustic waves can accelerate a part of protons through the Landau resonance. Our simulation results not only uncover the evolution pattern of whistler waves during the parametric decay in a two-dimensional regime but also propose a potential nonlinear physical process related to whistler waves in the Earth's magnetosphere. *Published by AIP Publishing.* https://doi.org/10.1063/1.5037763

I. INTRODUCTION

Whistler mode waves are intense electromagnetic emissions in the Earth's magnetosphere, which are well known for their significant role in regulating electron populations in the Van Allen radiation belt.[1,2] They have been commonly accepted to be mainly responsible for enhancements of relativistic electron fluxes in the Earth's radiation belt during geoactive periods[3–5] and precipitation of lower-energy ($\sim 10\,\mathrm{keV}$) electrons into the Earth's atmosphere.[6–8] Whistler mode waves have been thoroughly studied in the linear or quasi-linear regime since the past few decades,[9–11] but now nonlinear physical processes related to whistler mode waves are attracting more and more attention. The remarkable frequency chirping of whistler mode chorus waves has been widely believed to be caused by nonlinear interactions between whistler waves and resonant electrons.[12–15] Multiband chorus waves detected by THMIS satellites are well explained by the lower band cascade, which involves the nonlinear coupling between the electrostatic and electromagnetic components of lower band chorus waves.[16,17] Besides, the resonant interaction between whistler mode waves has also been reported in the Earth's magnetosphere[18] and then reproduced by full particle simulations.[19]

Another interesting nonlinear physical process is the parametric decay of whistler mode waves, which involves a backward propagating whistler mode wave and an ion acoustic mode.[20] Based on Van Allen Probes waveform data, Agapitov *et al.*[21] have reported a whistler wave event involving the parametric decay, which could be a potential source of time domain structures (TDS). With a one-dimensional particle-in-cell (PIC) simulation model, Ke *et al.*[22] have successfully reproduced the parametric decay of parallel whistler mode waves, which is quite consistent with the previous theoretical works.[20] However, the parametric decay of oblique whistler waves still remains unknown. In this letter, we have investigated the parametric decay of whistler mode waves in the Earth's magnetosphere with a two-dimensional (2-D) particle-in-cell (PIC) simulation model. Unexpectedly, the parametric decay can occur not only along the propagating direction of pump whistler waves but also in the direction perpendicular to the background magnetic field. Moreover, the perpendicular decay can excite a family of oblique whistler mode waves.

II. SIMULATION MODEL AND INITIAL SETUP

The PIC simulation model is a powerful tool to study nonlinear physical processes in space plasma.[17,23,24] A 2-D PIC simulation model with periodic boundary conditions is utilized to study the parametric decay of oblique whistler

a)Email: gaoxl@mail.ustc.edu.cn

waves, which allows three-dimensional electromagnetic fields and velocities but only two-dimensional spatial variations in the $x - y$ plane. The background magnetic field $\mathbf{B}_0$ is lying in the $x - y$ plane and with an angle θ with respect to the x axis. The simulation model is performed in a homogenous and collisionless electron-proton plasma. Both electrons and protons satisfy Maxwellian velocity distribution, and the electron beta is $\beta_e = 0.01$. Here, a smaller mass ratio between proton and electron $m_i/m_e = 400$ is chosen just to save computation resources. The system is initialized by launching a pump whistler wave along the x axis, which means that its wave normal angle is set as θ. With the same method as described by Gao *et al.*,[17] the pump whistler wave is initially set up by assigning fluctuating wave fields on each grid and fluctuating bulk velocities to each particle based on the linear theory model, i.e., WHAMP.[25]

In the simulation model, the units of time and space are the inverse of electron gyrofrequency Ω_e^{-1} and electron inertial length λ_e ($\lambda_e = c/\omega_{pe}$, where c and ω_{pe} are the light speed and plasma frequency), respectively. The number of grid cells is $n_x \times n_y = 512 \times 512$, and their total length in either x or y direction is given by $L = 5\lambda_w$, where λ_w is the wave length of the pump whistler wave. For each species, there are on average 1000 superparticles per cell. The time step is $\Delta t = 0.01\Omega_e^{-1}$. If we assume the background magnetic field and plasma density to be $B_0 \approx 100$ nT and $n_0 \approx 2.4\,\mathrm{cm}^{-3}$, which are typical values at L-shell ≈ 6 in the Earth's magnetosphere, then the ratio of the plasma frequency to electron gyrofrequency will be given as $\omega_{pe}/\Omega_e \approx 5$. Six simulation runs are performed in this study, whose parameters are listed in Table I.

III. SIMULATION RESULTS

The overview of nonlinear evolution of the pump whistler wave for Run 1 is shown in Fig. 1, which presents the time evolution of (a) magnetic fluctuations $\delta B_z^2/B_0^2$ of the pump whistler wave (solid line) and all other excited waves (dotted line) and (b) ion density fluctuations $\delta n_i^2/n_0^2$, respectively. Here, we have excluded the density fluctuations associated with the pump whistler wave in Fig. 1(b). In Fig. 1(a), the pump whistler wave is unstable to the parametric decay, and its magnetic amplitude gradually decreases with the time. Meanwhile, there are extra electromagnetic waves excited from the noise level in this system, which saturate at about $2500\,\Omega_e^{-1}$. Interestingly, those excited wave modes

TABLE I. Simulation parameters.[a]

Run	$k_0\lambda_e$	ω_0/Ω_e	θ (°)	$\delta B_{z0}/B_0$	T_{e0}/T_{i0}
1	0.92	0.4	30	0.02	25
2	0.72	0.3	30	0.02	25
3	1.13	0.4	45	0.02	25
4	0.92	0.4	30	0.05	25
5	0.92	0.4	30	0.01	1
6	0.82	0.4	0	0.05	25

[a]k_0 and ω_0 are the wave number and frequency of the pump wave, and δB_{z0} is the initial magnetic amplitude of the pump wave in the z direction. T_{e0} and T_{i0} are the initial electron and proton temperature, respectively.
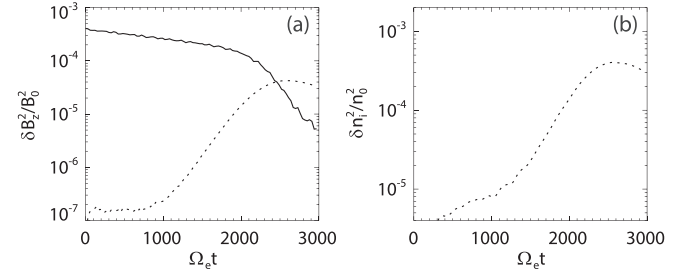
FIG. 1. Time evolution of (a) magnetic fluctuations $\delta B_z^2/B_0^2$ of the pump whistler wave (solid line) and all other excited waves (dotted line) and (b) excited ion density fluctuations $\delta n_i^2/n_0^2$ for Run 1, respectively.

experience two growth stages, which can be roughly divided by the time of $\sim 1000\,\Omega_e^{-1}$ (dotted line). The density fluctuations in Fig. 1(b) exhibit a similar evolution pattern, which begin to increase at the very beginning and then gain a more rapid growth from $\sim 1000\,\Omega_e^{-1}$ to the saturation stage.

Figure 2 presents the detailed spectra during the parametric decay, showing the power spectra of (a) and (b) magnetic fluctuations $\delta B_z/B_0$ and (c) and (d) ion density fluctuations $\delta n_i/n_0$ in the $k_x - k_y$ space at $\Omega_e t = 400$ and $\Omega_e t = 2500$ for Run 1, respectively. The two times are chosen to represent two distinct stages shown in Fig. 1. The parallel and perpendicular directions with respect to the background magnetic field have been marked by black solid lines. For separating the forward and reverse propagating modes in the $k_x - k_y$ space, we obtain the power spectra in Figs. 2(a) and 2(b) through the spatio-temporal Fourier analysis ($k - \omega$), which will also be used to calculate the frequencies of these modes. At $\Omega_e t = 400$, besides the pump whistler wave ($k_0 = 0.92\lambda_e^{-1}$ and $\omega_0 = 0.4\Omega_e$), there are two extra wave modes propagating
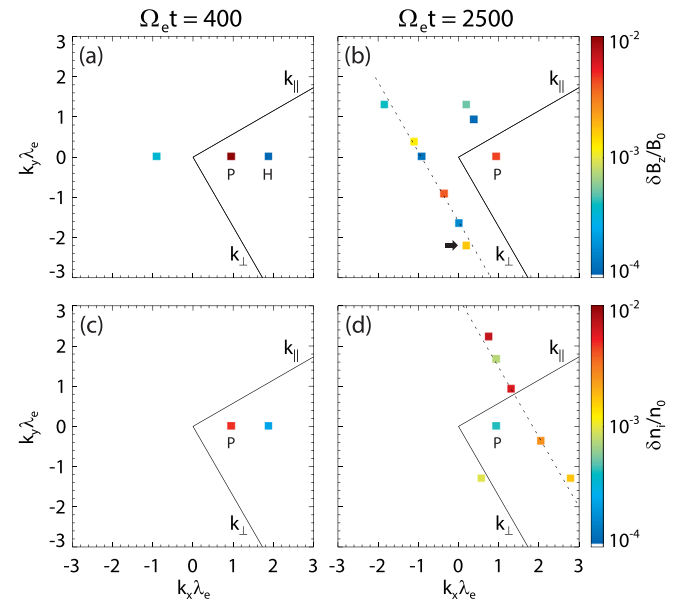
FIG. 2. The power spectra of (a) and (b) magnetic fluctuations $\delta B_z/B_0$ and (c) and (d) ion density fluctuations $\delta n_i/n_0$ in the $k_x - k_y$ space at $\Omega_e t = 400$ and $\Omega_e t = 2500$ for Run 1, respectively. The black solid lines denote the parallel ($k_{\parallel}$) and perpendicular ($k_{\perp}$) directions with respect to $\mathbf{B}_0$, and the dotted lines along the perpendicular direction are plotted as a reference. "P" and "H" mark the pump wave and its second harmonic, and the black arrow marks the most oblique whistler mode.

along the x axis in Fig. 2(a). One is identified as a backward whistler wave ($k = -0.92\lambda_e^{-1}$) at $\omega \approx 0.4\Omega_e$, which should be generated through the parametric decay of the pump whistler wave. Since a forward ion acoustic wave ($k_s = 1.84\lambda_e^{-1}$) at a very small frequency $\omega_s \approx 0$ is excited along the x axis [Fig. 2(c)], these three wave modes satisfy the resonant condition very well, i.e., $k_0 = k + k_s$ and $\omega_0 = \omega + \omega_s$. The other is identified as the second harmonic of the pump whistler wave, which is caused by the coupling between the electromagnetic and electrostatic components of the pump whistler wave.[17] This decay process of the pump whistler wave along its propagating direction in the first stage is quite similar to that of a parallel whistler wave in 1-D simulations.[22]

Surprisingly, at $\Omega_e t = 2500$, besides the backward whistler wave excited at the first stage, a family of wave modes at different propagation angles is generated in the system [Fig. 2(b)]. These wave modes are found to have different perpendicular wavenumbers $k_\perp$ but nearly the same parallel wavenumber $k_\parallel \approx -0.8\lambda_e^{-1}$ and wave frequency $\omega \approx 0.4\Omega_e$, which are revealed to be whistler waves. Similarly, the ion density spectrum also exhibits a family of ion density modes at different perpendicular wavenumbers $k_{s\perp}$ but nearly the same parallel wavenumber $k_{s\parallel} \approx 1.6\lambda_e^{-1}$ [Fig. 2(d)], whose wave frequencies are very small. Further analysis indicates that the generated whistler waves ($k_\parallel \approx -0.8\lambda_e^{-1}$, $k_\perp$), excited ion density modes ($k_{s\parallel} \approx 1.6\lambda_e^{-1}$, $k_{s\perp}$), and pump whistler wave ($k_{0\parallel} = 0.8\lambda_e^{-1}$, $k_{0\perp} = 0.46\lambda_e^{-1}$) satisfy the resonant condition

$$k_{0\parallel} = k_\parallel + k_{s\parallel} \tag{1}$$

and

$$k_{0\perp} = k_\perp + k_{s\perp}. \tag{2}$$

According to the three-wave resonant condition, the presence of the perpendicular wavenumber in the pump wave leads to nonzero perpendicular wavenumber in at least one of the daughter whistler waves and excited ion acoustic waves. Along the background magnetic field, the excited modes subject to the maximum growth rate of the decay instability have a given parallel wavenumber. However, a series of different perpendicular wavenumbers in excited modes are observed due to no similar constraint. Moreover, the resonant condition is satisfied by not only wavenumbers but wave frequencies. Therefore, for an oblique whistler wave, the parametric decay first takes place along its propagating direction, and then, the stronger perpendicular decay will occur. Meanwhile, the significant highly oblique whistler waves are also detected in Fig. 2(b), whose wave normal angles can even reach up to their resonant cone angle $\sim 66°$ (black arrow).

Figure 3 displays the spatial distributions of (a) magnetic fluctuations $\delta B_z/B_0$ and (b) ion density fluctuations $\delta n_i/n_0$ at $\Omega_e t = 2500$ for Run 1. The background magnetic field is denoted by white lines. Initially, the pump whistler wave is injected in this system, which has five sinusoidal waveforms along the x axis (not shown). However, at the saturation stage ($\Omega_e t = 2500$), we find that both magnetic and ion density
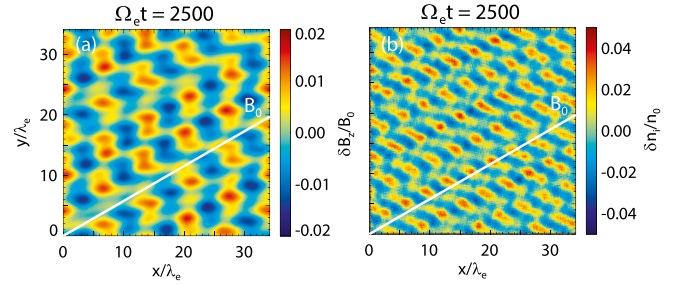
FIG. 3. Spatial distributions of (a) magnetic fluctuations $\delta B_z/B_0$ and (b) ion density fluctuations $\delta n_i/n_0$ at $\Omega_e t = 2500$ for Run 1. The background magnetic field $\mathbf{B}_0$ is denoted by white lines.

fluctuations have strong perpendicular components in Figs. 3(a) and 3(b), which is consistent with the intense perpendicular decay of the pump whistler wave [Figs. 2(b) and 2(d)]. Besides, magnetic fluctuations still show five clear waveforms along the background magnetic field in Fig. 3(a), meaning that those generated wave modes have nearly the same parallel wave number. Moreover, since many wave modes have been excited with different wave numbers, the waveforms shown in Figs. 3(a) and 3(b) have been strongly modulated, which are far away from a sinusoidal pattern.

Furthermore, we study the effects of the wave frequency and wave normal angle on the parametric decay of oblique whistler waves. Figure 4(a) presents the time evolution of excited ion density fluctuations $\delta n_i^2/n_0^2$ for Run 1 (dotted line), Run 2 (dashed line), and Run 3 (solid line), while Figs. 4(b) and 4(c) display the power spectra of magnetic fluctuations $\delta B_z/B_0$ at $\Omega_e t = 400$ and 2500 for Run 3. Here, the density fluctuations associated with the pump whistler wave are excluded in Fig. 4(a). Comparing Runs 1 and 2, they experience a similar pattern of the parametric decay just as shown in Fig. 2. However, the parametric decay in Run 2 is weaker than that in Run 1, since the pump wave in Run 2 has a smaller frequency. While, although the wave normal angle of the pump whistler wave in Run 3 is larger than that in Run 1, the parametric decay has nearly the same growth rate for both runs as displayed in Fig. 4(a). In Figs. 4(b) and 4(c), we also find a similar evolution pattern of the pump wave, but there are more significant highly oblique whistlers excited for the more oblique pump wave [Fig. 4(c)].

The effect of the wave amplitude on the parametric decay of nonparallel whistler waves is also considered. Figure 5(a) describes the time evolution of excited ion density fluctuations $\delta n_i^2/n_0^2$, and Figs. 5(b) and 5(c) illustrate the spectra of magnetic fluctuations $\delta B_z/B_0$ at $\Omega_e t = 400$ and 700 for Run 4. As expected, the ion density fluctuations in Run 4 increase more rapidly and saturate at a higher level compared with Run 1, which suggests that the pump wave with a larger amplitude tends to have a larger growth rate for the parametric decay. The decay process of the pump whistler wave in Run 4 also shows a similar pattern, which first takes place in the propagating direction of the pump wave [Fig. 5(b)] and then develops in the perpendicular direction [Fig. 5(c)].

Runs 1–4 have exhibited a clear evolution pattern of oblique whistler waves during the parametric decay, however, we
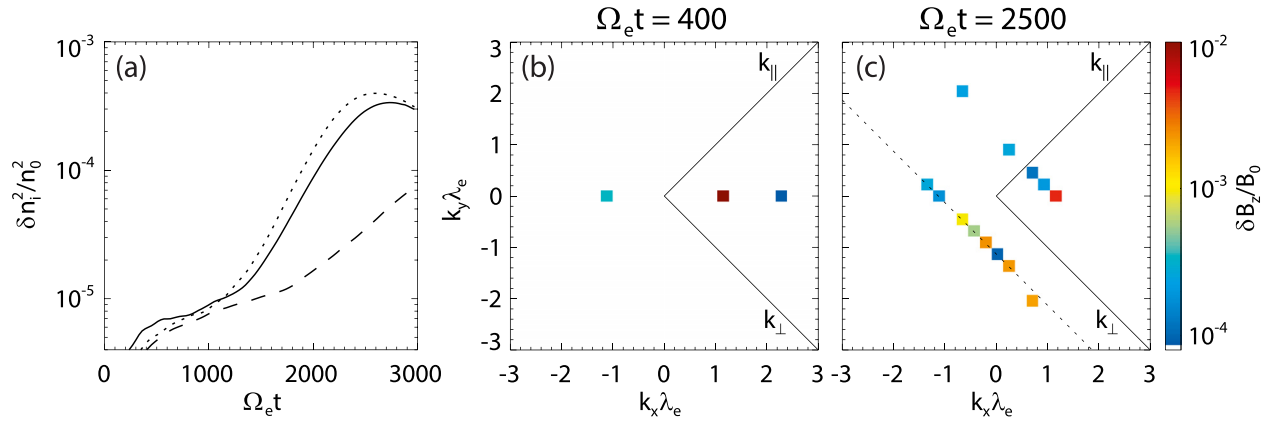
FIG. 4. Time evolution of (a) excited ion density fluctuations $\delta n_i^2/n_0^2$ for Run 1 (dotted line), Run 2 (dashed line), and Run 3 (solid line) and the power spectra of (b) and (c) magnetic fluctuations $\delta B_z/B_0$ at $\Omega_e t = 400$ and 2500 for Run 3.
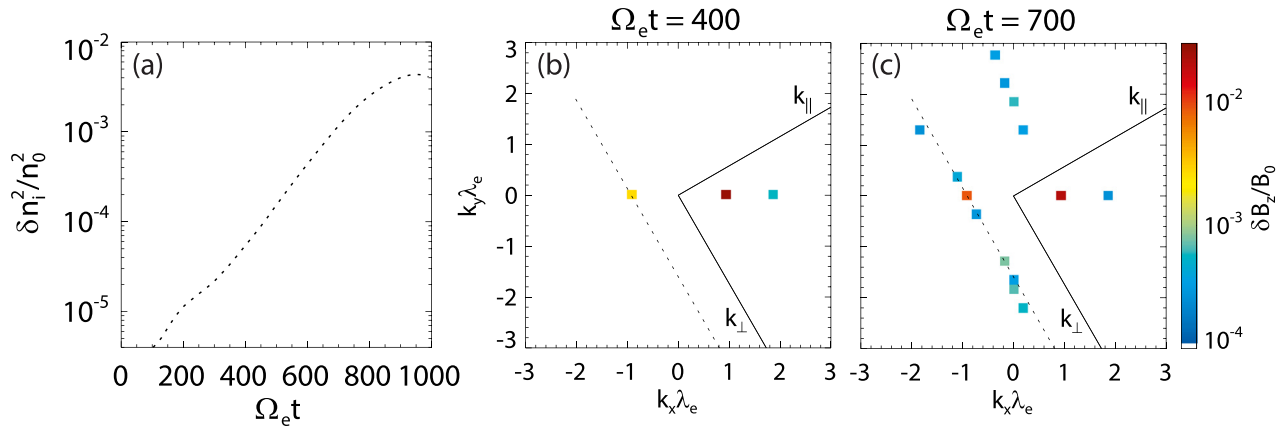
FIG. 5. The temporal evolution of (a) excited ion density fluctuations $\delta n_i^2/n_0^2$ and the power spectra of (b) and (c) magnetic fluctuations $\delta B_z/B_0$ at $\Omega_e t = 400$ and 700 for Run 4.

further perform Run 5 by choosing smaller $T_{e0}/T_{i0} = 1$ and $\delta B_{z0}/B_0 = 0.01$, which are more realistic in the Earth's magnetosphere. Figure 6 shows (a) the temporal evolution of ion density fluctuations $\delta n_i^2/n_0^2$ exclusive of the component associated with the pump whistler wave and the power spectra of (b, c) magnetic fluctuations $\delta B_z/B_0$ at $\Omega_e t = 500$ and 3100 for Run 5. As shown in Fig. 6(a), the ion density fluctuations can be also observed to increase from the very beginning, suggesting the occurrence of the parametric decay. However, the ion density fluctuations saturate at a low level, which is mainly caused by the enhanced damping of ion acoustic modes in the case of $T_{e0}/T_{i0} = 1$. The pump whistler wave in Run 5 also undergoes a similar decay process, which first occurs in the propagating direction of the pump wave [Fig. 6(b)] and then takes place in the perpendicular direction [Fig. 6(c)]. But the growth rate of the parametric decay is small and the saturated amplitudes of daughter whistler waves are about 1–2 orders smaller than that of the pump whistler wave.

Besides, we also carry out a 2-D simulation run (Run 6) for the parallel whistler wave. The simulation results are given in Fig. 7, which presents the power spectra of (a) magnetic fluctuations $\delta B_z/B_0$ and (b) ion density fluctuations $\delta n_i/n_0$ at $\Omega_e t = 1000$, (c) the scatter plot in the $(x, v_{\parallel})$ plane, and (d) the parallel velocity distribution for protons at $\Omega_e t = 1000$ for Run 6. Interestingly, we find that the parallel

whistler wave can also drive fairly strong daughter whistler waves [Fig. 7(a)] and ion acoustic waves [Fig. 7(b)] along the perpendicular direction through the parametric decay, which may suggest that the parametric decay of whistler waves could be a multi-dimensional (two or three) process. The phase velocity of ion acoustic waves can be estimated as $v_p = \sqrt{T_e/m_i} = 5v_{ti}$, where v_{ti} is the thermal velocity of protons. As shown in Fig. 7(c), the generated ion acoustic waves can accelerate a part of protons through the Landau resonance, which can also be seen in the parallel velocity distribution function of protons [the flat top at $\sim 5\, v_{ti}$ in Fig. 7(d)].

IV. CONCLUSION AND DISCUSSION

By employing a 2-D PIC simulation model, we have studied the parametric decay of oblique whistler waves in the Earth's magnetosphere. The parametric decay of whistler waves first occurs along the propagating direction, which involves a backward daughter whistler wave and a forward ion acoustic mode. This is quite similar to the parametric decay of parallel whistler waves in 1-D simulations.[22] Surprisingly, the parametric decay will then take place in the perpendicular direction, which can generate a family of whistler waves along the perpendicular direction with the nearly same parallel wave number. Meanwhile, the highly
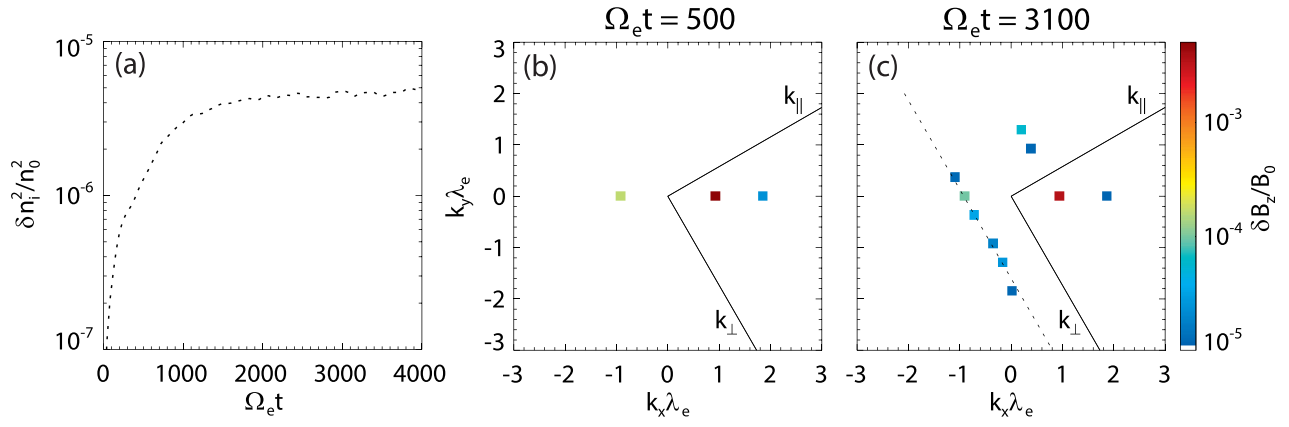
FIG. 6. (a) The temporal evolution of excited ion density fluctuations $\delta n_i^2/n_0^2$ and the power spectra of (b) and (c) magnetic fluctuations $\delta B_z/B_0$ at $\Omega_e t = 500$ and 3100 for Run 5.
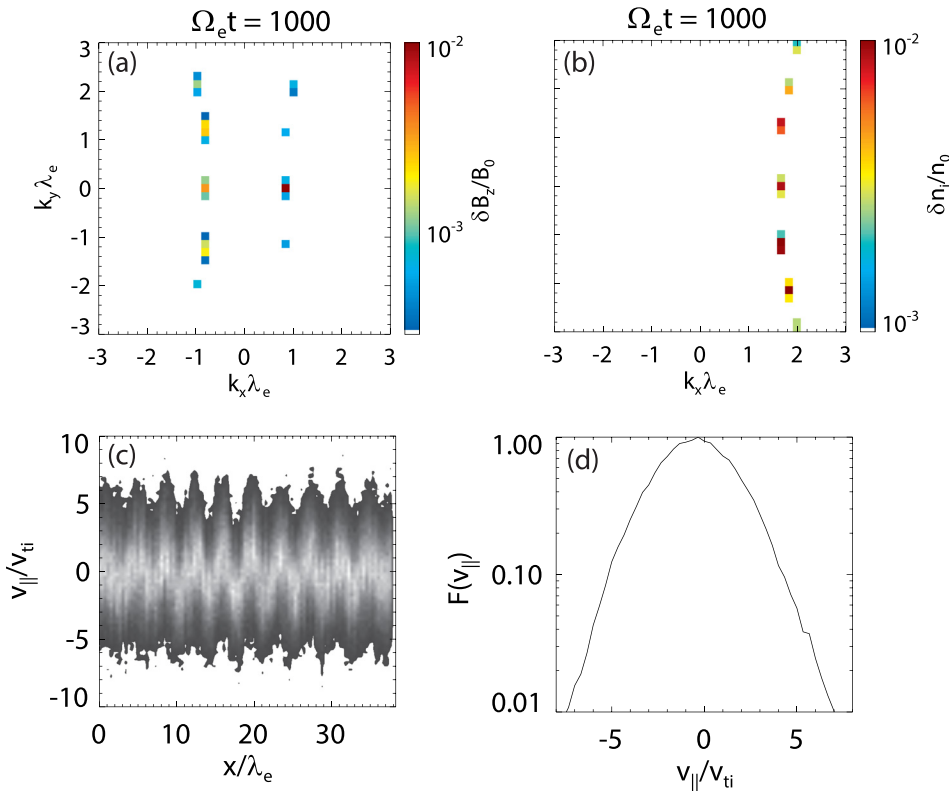
FIG. 7. The power spectra of (a) magnetic fluctuations $\delta B_z/B_0$ and (b) ion density fluctuations $\delta n_i/n_0$ at $\Omega_e t = 1000$. (c) The scatter plot in the $(x, v_{\parallel})$ plane and (d) the parallel velocity distribution for protons at $\Omega_e t = 1000$ for Run 6.

oblique whistler waves will also be excited during this perpendicular decay, whose wave normal angle can even reach up to the resonant cone angle. The parametric decay of oblique whistler waves is very similar to that of oblique Alfven waves.[26] Moreover, the parametric decay tends to be stronger for the pump whistler wave with a larger frequency or larger amplitude. But the growth rate of the parametric decay has little change when the wave normal angle of the pump whistler wave varies within a limited range. Besides, 2-D simulation results reveal that the parallel whistler wave can also experience the similar decay process, which may suggest that the parametric decay of whistler waves should be a multi-dimensional (two or three) process in nature. During the parametric decay, the generated ion acoustic waves can accelerate a part of protons through the Landau resonance,

which may play a role in turning off the decay process by saturating the ion acoustic waves.

Nonlinear physical processes related to whistler mode waves are now becoming a hot topic because of their significant role in reshaping whistler spectra in the Earth's magnetosphere. The lower band cascade, involving the nonlinear coupling between the electrostatic and electromagnetic components of lower band chorus waves, may contribute to the formation of banded spectral structures of chorus waves.[16] The resonant interactions between whistler waves have also been detected by THEMIS satellites in the Earth's magnetosphere.[18] In our simulation results, oblique whistler waves with a small magnetic amplitude are found to be unstable to the parametric decay, which will excite a family of whistler waves and ion density modes along the perpendicular

direction. This suggests that whistler waves in the Earth's magnetosphere may also experience the parametric decay during their propagation, but it still requires the further observational support.

With respect to oblique whistler waves in the Earth's magnetosphere, there are several mechanisms proposed to explain their generation. Both the linear theory and PIC simulations have shown that oblique whistler waves will be excited by anisotropic electrons if their parallel beta is very small (<0.02).[27,28] Mourenas *et al.*[29] pointed out that oblique whistler waves can be excited by electron beams through the either Landau or cyclotron resonance, which has also been further supported by a statistical work by Gao *et al.*[30] Based on THEMIS observations, Gao *et al.*[18] reported several chorus events involving nonlinear wave-wave couplings, which is also considered as a potential generation mechanism of oblique whistler waves. With 2-D PIC simulations, Fu *et al.*[19] have successfully reproduced oblique whistler waves through nonlinear resonant interactions between whistler waves. Our simulation results show that oblique whistler waves will also be excited during the parametric decay, whose wave normal angle can even reach up to the resonant cone angle and magnetic amplitudes are quite significant [Fig. 2(b)]. Therefore, our study also provides a possible generation mechanism of highly oblique whistler waves in the Earth's magnetosphere.

ACKNOWLEDGMENTS

[1]D. Summers, B. Ni, and N. P. Meredith, "Timescales for radiation belt electron acceleration and loss due to resonant wave-particle interactions: 2. Evaluation for VLF chorus, ELF hiss, and electromagnetic ion cyclotron waves," J. Geophys. Res.: Space Phys. **112**, A04207, https://doi.org/10.1029/2006JA011993 (2007).

[2]R. M. Thorne, "Radiation belt dynamics: The importance of wave-particle interactions," Geophys. Res. Lett. **37**, L22107, https://doi.org/10.1029/2010GL044990 (2010).

[3]G. D. Reeves, H. E. Spence, M. G. Henderson, S. K. Morley, R. H. W. Friedel, H. O. Funsten, D. N. Baker, S. G. Kanekal, J. B. Blake, J. F. Fennell, S. G. Claudepierre, R. M. Thorne, D. L. Turner, C. A. Kletzing, W. S. Kurth, B. A. Larsen, and J. T. Niehof, "Electron acceleration in the heart of the Van Allen radiation belts," Science **341**, 991 (2013).

[4]R. M. Thorne, W. Li, B. Ni, Q. Ma, J. Bortnik, L. Chen, D. N. Baker, H. E. Spence, G. D. Reeves, M. G. Henderson, C. A. Kletzing, W. S. Kurth, G. B. Hospodarsky, J. B. Blake, J. F. Fennell, S. G. Claudepierre, and S. G. Kanekal, "Rapid local acceleration of relativistic radiation-belt electrons by magnetospheric chorus," Nature **504**, 411 (2013).

[5]D. Mourenas, A. V. Artemyev, O. V. Agapitov, and V. Krasnoselskikh, "Consequences of geomagnetic activity on energization and loss of radiation belt electrons by oblique chorus waves," J. Geophys. Res.: Space Phys. **119**, 2775–2796, https://doi.org/10.1002/2013JA019674 (2014).

[6]R. M. Thorne, B. Ni, X. Tao, R. B. Horne, and N. P. Meredith, "Scattering by chorus waves as the dominant cause of diffuse auroral precipitation," Nature **467**, 943 (2010).

[7]B. Ni, R. M. Thorne, Y. Y. Shprits, K. G. Orlova, and N. P. Meredith, "Chorus-driven resonant scattering of diffuse auroral electrons in nondipolar magnetic fields," J. Geophys. Res.: Space Phys. **116**, A06225, https://doi.org/10.1029/2011JA016453 (2011).

[8]Y. Nishimura, J. Bortnik, W. Li, R. M. Thorne, B. Ni, L. R. Lyons, V. Angelopoulos, Y. Ebihara, J. W. Bonnell, O. Le Contel, and U. Auster, "Structures of dayside whistler-mode waves deduced from conjugate diffuse aurora," J. Geophys. Res.: Space Phys. **118**, 664–673, https://doi.org/10.1029/2012JA018242 (2013).

[9]A. Artemyev, O. Agapitov, H. Breuillard, V. Krasnoselskikh, and G. Rolland, "Electron pitch-angle diffusion in radiation belts: The effects of whistler wave oblique propagation," Geophys. Res. Lett. **39**, L08105, https://doi.org/10.1029/2012GL051393 (2012).

[10]D. Mourenas, A. V. Artemyev, J.-F. Ripoll, O. V. Agapitov, and V. V. Krasnoselskikh, "Timescales for electron quasi-linear diffusion by parallel and oblique lower-band chorus waves," J. Geophys. Res.: Space Phys. **117**, A06234, https://doi.org/10.1029/2012JA017717 (2012).

[11]W. Li, R. M. Thorne, Q. Ma, B. Ni, J. Bortnik, D. N. Baker, H. E. Spence, G. D. Reeves, S. G. Kanekal, J. C. Green, C. A. Kletzing, W. S. Kurth, G. B. Hospodarsky, J. B. Blake, J. F. Fennell, and S. G. Claudepierre, "Radiation belt electron acceleration by chorus waves during the 17 March 2013 storm," J. Geophys. Res.: Space Phys. **119**, 4681–4693, https://doi.org/10.1002/2014JA019945 (2014).

[12]Y. Omura, M. Hikishima, Y. Katoh, D. Summers, and S. Yagitani, "Nonlinear mechanisms of lower-band and upper-band VLF chorus emissions in the magnetosphere," J. Geophys. Res. **114**, A07217, https://doi.org/10.1029/2009JA014206 (2009).

[13]X. Gao, W. Li, R. M. Thorne, J. Bortnik, V. Angelopoulos, Q. M. Lu, X. Tao, and S. Wang, "New evidence for generation mechanisms of discrete and hiss-like whistler mode waves," Geophys. Res. Lett. **41**, 4805–4811, https://doi.org/10.1002/2014GL060707 (2014).

[14]X. Tao, Q. Lu, S. Wang, and L. Dai, "Effects of magnetic field configuration on the day-night asymmetry of chorus occurrence rate: A numerical study," Geophys. Res. Lett. **41**, 6577–6582, https://doi.org/10.1002/2014GL061493 (2014).

[15]Y. Ke, X. L. Gao, Q. M. Lu, X. Y. Wang, and S. Wang, "Generation of rising-tone chorus in a two-dimensional mirror field by using the general curvilinear PIC code," J. Geophys. Res.: Space Phys. **122**, 8154–8165, https://doi.org/10.1002/2017JA024178 (2017).

[16]X. Gao, Q. Lu, J. Bortnik, W. Li, L. Chen, and S. Wang, "Generation of multiband chorus by lower band cascade in the Earth's magnetosphere," Geophys. Res. Lett. **43**, 2343–2350, https://doi.org/10.1002/2016GL068313 (2016).

[17]X. Gao, Y. G. Ke, Q. M. Lu, L. J. Chen, and S. Wang, "Generation of multiband chorus in the Earth's magnetosphere: 1-D PIC simulation," Geophys. Res. Lett. **44**, 618–624, https://doi.org/10.1002/2016GL072251 (2017).

[18]X. Gao, Q. Lu, and S. Wang, "First report of resonant interactions between whistler mode waves in the Earth's magnetosphere," Geophys. Res. Lett. **44**, 5269, https://doi.org/10.1002/2017GL073829 (2017).

[19]X. Fu, S. P. Gary, G. D. Reeves, D. Winske, and J. R. Woodroffe, "Generation of highly oblique lower band chorus via nonlinear three-wave resonance," Geophys. Res. Lett. **44**, 9532, https://doi.org/10.1002/2017GL074411 (2017).

[20]D. W. Forslund, J. M. Kindel, and E. L. Lindman, "Parametric excitation of electromagnetic waves," Phys. Rev. Lett. **29**, 249 (1972).

[21]O. V. Agapitov, V. Krasnoselskikh, F. S. Mozer, A. V. Artemyev, and A. S. Volokitin, "Generation of nonlinear electric field bursts in the outer radiation belt through the parametric decay of whistler waves," Geophys. Res. Lett. **42**, 3715–3722, https://doi.org/10.1002/2015GL064145 (2015).

[22]Y. Ke, X. L. Gao, Q. M. Lu, and S. Wang, "Parametric decay of a parallel propagating monochromatic whistler wave: Particle-in-cell simulations," Phys. Plasmas **24**, 012108 (2017).

[23]X. Fu, Q. M. Lu, and S. Wang, "The process of electron acceleration during collisionless magnetic reconnection," Phys. Plasmas **13**, 012309 (2006).

[24]S. Lu, V. Angelopoulos, and H. Fu, "Suprathermal particle energization in dipolarization fronts: Particle-in-cell simulations," J. Geophys. Res.: Space Phys. **121**, 9483–9500, https://doi.org/10.1002/2016JA022815 (2016).

[25]K. Rönnmark, "WHAMP: Waves in homogeneous, anisotropic, multicomponent plasmas," Report No. 179, Kiruna Geophysics Institute, Kiruna, Sweden, 1982.

[26]L. Matteini, S. Landi, L. Del Zanna, M. Velli, and P. Hellinger, "Parametric decay of linearly polarized shear Alfvén waves in oblique propagation: One and two-dimensional hybrid simulations," Geophys. Res. Lett. **37**, L20101, https://doi.org/10.1029/2010GL044806 (2010).

[27]S. P. Gary, K. Liu, and D. Winske, "Whistler anisotropy instability at low electron β: Particle-in-cell simulations," Phys. Plasmas **18**, 082902 (2011).

[28]X. An, C. Yue, J. Bortnik, V. Decyk, W. Li, and R. M. Thorne, "On the parameter dependence of the whistler anisotropy instability," J. Geophys. Res.: Space Phys. **122**, 2001–2009, https://doi.org/10.1002/2017JA023895 (2017).

[29]D. Mourenas, A. Artemyev, O. Agapitov, V. Krasnoselskikh, and F. S. Mozer, "Very oblique whistler generation by low-energy electron streams," J. Geophys. Res.: Space Phys. **120**, 3665–3683, https://doi.org/10.1002/2015JA021135 (2015).

[30]X. Gao, D. Mourenas, W. Li, A. V. Artemyev, Q. Lu, X. Tao, and S. Wang, "Observational evidence of generation mechanisms for very oblique lower band chorus using THEMIS waveform data," J. Geophys. Res.: Space Phys. **121**, 6732–6748, https://doi.org/10.1002/2016JA022915 (2016).